Catalysis Today 161 (2011) 153–162

Contents lists available at ScienceDirect

Catalysis Today

journal homepage: www.elsevier.com/locate/cattod

Photocatalytic removal of s-triazines: Evaluation of operational parameters

M.J. López-Muñoz*, J. Aguado, A. Revilla

Department of Chemical and Environmental Technology, ESCET, Universidad Rey Juan Carlos, C/Tulipán s/n, 28933 Móstoles, Madrid, Spain

ARTICLE INFO

Article history:
Available online 24 November 2010

Keywords:
Photocatalysis
Atrazine
Simazine
Factorial design of experiments

ABSTRACT

The photocatalytic degradation of atrazine (2-chloro-4-ethylamino-6-isopropylamino-1,3,5-triazine) and simazine (2-chloro-4,6-diethylamino-1,3,5-triazine) herbicides widely used in agriculture has been investigated. Experimental design methodology was used to assess the influence of pH and TiO_2 concentration and the efficiency of the process. The results indicated that in the experimental domain investigated TiO_2 concentration was the most significant factor in contrast to the scarce influence shown by the initial pH. The mechanism of atrazine and simazine photocatalytic degradation was studied under the experimental conditions determined as optimal. No full mineralization of atrazine or simazine was achieved. The main intermediates occurring during the reaction were identified by high performance liquid chromatography (HPLC). Based on the concentration profile of intermediates formed during the treatment a degradation pathway is proposed for each herbicide. The toxicity along the reaction was monitored by means of luminescence bioassays using *Vibrio fischeri*. The inhibition percentage decreases with the irradiation times what can be associated with the formation of highly hydroxylated intermediates.

1. Introduction

Atrazine (2-chloro-4-ethylamino-6-isopropylamino-1,3,5-triazine) and simazine (2-chloro-4,6-diethylamino-1,3,5-triazine) are some of the herbicides most widely used over the last 30 years for selective broad-leaved and grassy weeds control on a variety of crops such as corn, sugarcane, and pineapple [1]. Due to their relatively high persistence and mobility in soils these s-triazines can contaminate surface and ground waters where, in addition to their direct toxic effects, their phytotoxicity may constitute a major environmental problem. It has been probed that many zooplankton species show a reduction in reproduction and growth when their ecosystems are exposed to triazines [2].

In general, s-triazines are not readily biodegradable and rather resistant to conventional treatment methods therefore difficulting detoxification water processes. Concerns about the widespread water pollution and the repeatedly presence of atrazine and simazine residues in drinking water have led to bans or severe restrictions for their use in many countries. In the EU both herbicides are included in the list of priority substances given in the Directives 2000/60/EC and 2008/105/EC of the European Parliament and of the Council on environmental quality standards in the field of water policy [3].

Heterogeneous photocatalysis with titanium dioxide has been demonstrated as a good alternative to the conventional methods for the treatment of effluents contaminated with a variety of pesticides [4,5]. Previous studies have shown that photocatalytic degradation of triazine herbicides takes place by several steps leading to formation of cyanuric acid (trihydroxy s-triazine) as final stable product [6–11]. The high stability of the s-triazine ring prevents a further degradation to achieve the full mineralization even upon addition to the solution of an oxidant such as peroxydisulphate [7]. The majority of research done to study the influence of reaction parameters on the efficiency of the photocatalytic degradation of triazines has been carried out by univariate approaches (one variable is changed at time maintaining the others constant). An interesting alternative to this methodology is the experimental factorial design, a statistical tool that allows the simultaneous change of several variables [12,13]. To the best of our knowledge, only Héquet et al. [8] have reported a multivariate analysis on atrazine photocatalytic degradation, but no similar studies have been described for simazine.

The present work focuses on the photocatalytic degradation of atrazine and simazine in water using suspended TiO_2. The main aspects investigated have been: (i) the optimization of the degradation procedure by means of a factorial design of experiments studying the simultaneous effect of pH and TiO_2 concentration on the herbicide degradation rate, (ii) the identification of intermediate products in order to establish a tentative reaction pathway for both triazines and clarify some dissimilarities found in the literature and (iii) the evaluation of the toxicity along the pho-

* Corresponding author. Tel.: +34 914887464; fax: +34 914887068.
E-mail address: mariajose.lopez@urjc.es (M.J. López-Muñoz).

0920-5861/$ – see front matter © 2010 Elsevier B.V. All rights reserved.
doi:10.1016/j.cattod.2010.10.076

tocatalytic reactions by means of luminescence bioassays using *Vibrio fischeri*.

2. Materials and methods

2.1. Chemicals

Table 1 displays the chemical structure, nomenclature and acronyms of the organics according to the nomenclature developed by Cook and Hütter [14] and Nélieu et al. [15] to identify s-triazine compounds. All were of analytical grade and used as received. Atrazine 99% (2-chloro-4-ethylamino-6-isopropylamino-s-triazine), simazine 99.5% (2-chloro-4,6-diethylamino-s-triazine), desisopropyl-atrazine 95% (2-chloro-4-ethylamino-6-amino-s-triazine), desethyl-atrazine 99% (2-chloro-4-amino-6-isopropyl-amino-s-triazine), hydroxy-atrazine 96% (2-hydroxy-4-ethyl-amino-6-isopropylamino-s-triazine), desisopropyl-2-hydroxy-atrazine 95% (2-hydroxy-4-ethylamino-6-amino-s-triazine) and hydroxy-simazine 99.5% (2-hydroxy-4,6-diethylamino-s-triazine) were purchased from Riedel-de Häen. The standard desethyl-2-hydroxy-atrazine 99% (2-hydroxy-4-amino-6-isopropylamino-s-triazine) was obtained from Fluka. Standards cyanuric acid 98% (2,4,6-trihydroxy-s-triazine) and desethyl-desisopropyl-atrazine 95% (2-chloro-4,6-diamino-s-triazine) were acquired from Aldrich. Ammeline 95% (2-hydroxy-4,6-diamino-1,3,5-triazine) and ammelide (2,4-dihydroxy-6-amino-1,3,5-triazine) were purchased from ABCR. All standard solutions were prepared using organic-free deionized water (Milli-Q). Titanium dioxide P-25 supplied by Degussa was used as photocatalyst. It is a non-porous solid for which a BET surface area of 50 m^2 and mean particle size of ca. 30 nm were measured. It contains anatase and rutile crystalline phases in a ratio 4:1. In all experiments initial concentrations of 25 and 5 mg L^{-1} were set for atrazine and simazine, respectively.

2.2. Photocatalysis procedure

Photocatalytic reactions were carried out in a batch Pyrex reactor of 1 L effective solution volume. Irradiations were carried out using a 150 W medium pressure mercury lamp (Heraeus TQ-150), placed inside a Pyrex jacket and provided with a cooling tube through which an aqueous solution of copper sulphate (0.01 M) was circulated to prevent the overheating of the suspension and to cut off the radiation below 300 nm. The initial pH values of the herbicides solutions were adjusted with H_2SO_4 0.1 M or NaOH 0.1 M. Prior to irradiation, the suspension of triazine and catalyst was air saturated and equilibrated by magnetic stirring for 20 min in the dark to ensure complete equilibration of adsorption/desorption of the organic compound on the catalyst surface. Continuous air bubbling and stirring were maintained through the reaction. Aliquots were taken at time intervals, following filtration through 0.22 μm Nylon filters in order to remove the suspended TiO_2 particles before being analyzed.

2.3. Analysis

2.3.1. Liquid chromatography

High performance liquid chromatography (Varian Polaris Prostar 320) system equipped with UV–VIS detector was used to identify and quantify the products obtained in the photocatalytic reactions. The separation was performed using a Synergi 4 μ MAX-RP column. CEIT, CEET, ACIT and ACET were eluted with a gradient of aqueous phosphate buffer (pH 7)–acetonitrile (55:45, v/v) to (35:65, v/v), at a flow rate of 0.5 ml min^{-1} and detection at 210 nm. Elution of the other components, EOIT, EEOT, AOIT, AEOT, CAAT, OAAT, OOAT and OOOT were carried out with a gradient of aqueous phosphoric acid buffer (pH 3)–acetonitrile (95:5, v/v) to (40:60, v/v), at a flow rate of 0.8 ml min^{-1} and UV detection at 205 nm.

2.3.2. Toxicity measurements

The toxicity evaluation of samples was performed with a Microtox Model 550 Toxicity Analyzer. The analysis is based on the measurement of the ability of the sample to inhibit the natural bioluminescence of the marine bacterium *Vibrio fischeri* (strain NRLL no. B-11177). The bacteria were in freeze-dried form (acquired from Gomensoro) and activated prior to use by NaCl (2%) reconstitution solution. Samples were tested in solution containing 2% sodium chloride in six dilutions. After 15 min of incubation at 15 °C light emission was recorded and compared with a toxic-free control. The percentage of inhibition was obtained following the established protocol using the Microtox calculation program.

2.3.3. Factorial experimental design

Multivariate experimental design was carried out following the methodology of response surface [13]. The software Statgraphics Plus 5.0 was used to obtain the polynomial equations and the response surfaces.

3. Results and discussion

Preliminary experiments were done without either titanium dioxide or UV irradiation to evaluate the extent of adsorption and photolysis of the herbicides under our experimental conditions. Dark adsorption was negligible for both compounds as no significant variations in concentration were found after 6 h. On the contrary, photolysis was shown to occur to some extent. After a time period of 1 h, degradation percentages of 15% and 25% were respectively observed for atrazine and simazine. Our results are significantly different from those reported by Héquet et al. [8] who found a half-life time of 2.3 min for the photolytic atrazine degradation using a TQ 150-Z2 Heraeus lamp. Dissimilarities can be mainly due to the differences in the irradiation set-up as we employed a combination of Pyrex and copper sulphate solution as filtering system instead of the quartz filter they used. On the other hand, the photolysis extent found for simazine is in accordance with the results obtained by Chu et al. [10] who also report a significant dependence of the process with wavelength in the 254–350 nm range.

The kinetics of atrazine and simazine degradation was significantly enhanced by irradiation in the presence of titanium dioxide as catalyst following a pseudo-first order decay, in agreement with previous reports [6,9,10]. The effect of pH and titania concentration on the kinetics of the reaction were investigated by experimental design methodology as it allows to obtain the optimal conditions for the photocatalytic procedure from a minimum set of experiments. Based on preliminary experiments carried out in a wide domain of TiO_2 concentration from 0.05 to 3 g L^{-1} at the natural pH of the herbicide, a catalyst concentration ranging from 0.05 to 1.95 g L^{-1} and initial pH from 3 to 9 was selected for atrazine. For simazine, a TiO_2 concentration from 0.05 to 0.25 g L^{-1} and a pH interval 3–8 was fixed. Natural pH, i.e. 6.0 for atrazine and 5.5 for simazine, was chosen as central point in both cases.

In a first approach, a two-level factorial design consisting in four experiments (2^2) at the limits of the pH and TiO_2 intervals and three experiments at the central values of the two factors to determine the experimental error and any possible effects of curvature in the response surface were carried out. The analysis of the data obtained showed that the curvature was significant, indicating that a high-order model or response surface study was needed in order to uncover the behaviour of the significant factors [13]. Therefore, four experiments were performed in addition at the midpoints to

Table 1
Atrazine, simazine and main intermediates produced in the photocatalytic reaction.

Chemical and (common) name	Acronym[a]	Structure
2-Chloro-4-ethylamino-6-isopropylamino-1,3,5-triazine (atrazine)	CEIT	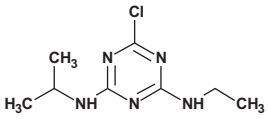
2-Chloro-4,6-diethylamino-1,3,5-triazine (simazine)	CEET	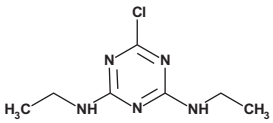
4-Ethylamino-2-hydroxy-6-isopropylamino-1,3,5-triazine	EOIT	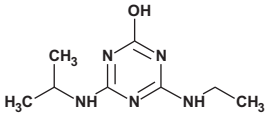
4,6-Diethylamino-2-hydroxy-1,3,5-triazine	EEOT	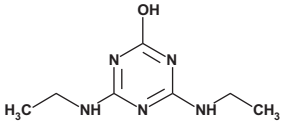
4-Amino-2-chloro-6-isopropylamino-1,3,5-triazine	ACIT	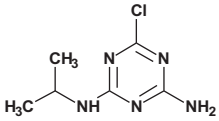
6-Amino-2-chloro-4-ethylamino-1,3,5-triazine	ACET	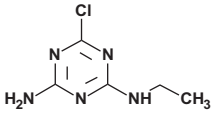
4-Amino-2-hydroxy-6-isopropylamino-1,3,5-triazine	AOIT	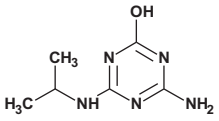
6-Amino-4-ethylamino-2-hydroxy-1,3,5-triazine	AEOT	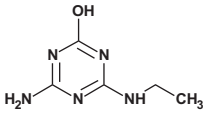
2-Chloro-4,6-diamino-1,3,5-triazine	CAAT	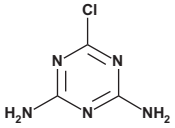
2-Hydroxy-4,6-diamino-1,3,5-triazine (ammeline)	OAAT	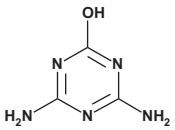
2,4-Dihydroxy-6-amino-1,3,5-triazine (ammelide)	OOAT	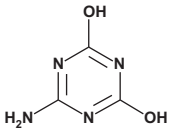
2,4,6-Trihydroxy-1,3,5-triazine (cyanuric acid)	OOOT	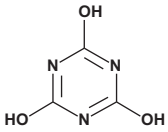

[a] A: amino, E: ethylamino, O: hydroxy, C: chloro, I: isopropylamino and T: triazine ring.

Table 2
Values and code levels of the experimental factors.

Component	Factors	Low level (−1)	Central level (0)	High level (+1)
Atrazine	pH	3.00	6.00	9.00
	$[TiO_2]/g\,L^{-1}$	0.05	1.00	1.95
Simazine	pH	3.00	5.50	8.00
	$[TiO_2]/g\,L^{-1}$	0.05	0.15	0.25

develop a full three level (3^2) factorial design (two variables and three levels).

The two factors (pH and TiO_2 concentration) were codified for each herbicide in three levels: low, medium and high, respectively, denoted as −1, 0, +1. The actual values and code levels of the experimental factors are displayed in Table 2.

Degradation percentages values achieved for each triazine after 6, 10 and 15 min of reaction were chosen as design response variables. Solving the matrix of data shown in Table 2, a quadratic polynomial equation in terms of the coded values of factors was obtained as follows:

$$Y = a_0 + b_1\mathrm{pH} + b_2[TiO_2] + b_{11}\mathrm{pH}^2 + b_{12}\mathrm{pH}\cdot[TiO_2] + b_{22}[TiO_2]^2 \quad (1)$$

where Y represents the triazine degradation (%) at the chosen time, a_0 is the independent coefficient, b_1 and b_2 are the linear coefficients for the variables pH and TiO_2 concentration, respectively, and b_{11}, b_{12} and b_{22} are the quadratic interaction terms.

3.1. Response surfaces of atrazine degradation

Response functions with the coefficients determined for the percentage of atrazine degradation at 6, 10 and 15 min (Y_1, Y_2 and Y_3, respectively) are given in Eqs. (2)–(4).

$$Y_1 = 37.9316 + 0.7667\mathrm{pH} + 10.5333[TiO_2] - 0.7789\mathrm{pH}^2 - 10.0789[TiO_2]^2 - 6.6750\mathrm{pH}\cdot[TiO_2] \quad (2)$$

$$Y_2 = 57.9632 + 1.9833\mathrm{pH} + 13.3167[TiO_2] - 2.3079\mathrm{pH}^2 - 13.1079[TiO_2]^2 - 9.4250\mathrm{pH}\cdot[TiO_2] \quad (3)$$

$$Y_3 = 72.1526 + 2.6833\mathrm{pH} + 14.5500[TiO_2] - 5.0816\mathrm{pH}^2 - 12.8816[TiO_2]^2 - 10.2500\mathrm{pH}\cdot[TiO_2] \quad (4)$$

Validation of the mathematical model was performed using the analysis of variance test (ANOVA) for every response function. In this test, the P-value of <0.05 for any factor indicates a significant effect of the corresponding variable on the response. Table 3 displays the experimental and predicted results for the three selected response factors.

The P-values calculated by the statistical model pointed out that only TiO_2 is a significant factor. Considering the first order effects of each variable and Eqs. (2)–(4) the response function coefficients indicate that pH and TiO_2 concentration have positive effects on the herbicide photocatalytic degradation therefore increasing these parameters favors the atrazine removal efficiency. However, the low b_1 value reveals the scarce influence of the pH on the process whereas, by contrast, the value of linear coefficient for TiO_2 concentration (b_2) indicates the significance of this variable.

Fig. 1 shows the relationship between the experimental and predicted values for each response factor. As it can be observed, the best accuracy corresponds to the values obtained at 6 min of irradiation (R^2 of 0.9537), whereas at higher response times a decrease in the goodness of fit to 0.8836 (10 min) and 0.8607 (15 min) is

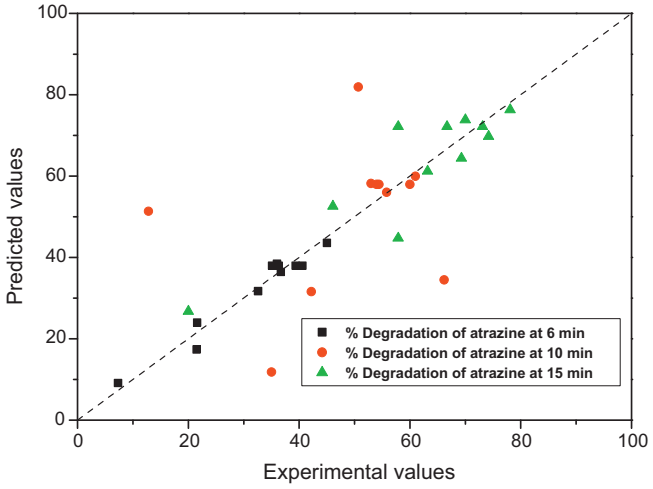

Fig. 1. Correlation between predicted and experimental values in the photocatalytic degradation of atrazine at different irradiation times.

obtained. Most likely, the intermediates formed as the reaction proceeds may account for this result by a competition against remaining atrazine for the active sites on the titania surface.

The overall interaction effects are displayed in Fig. 2, which shows 3D and 2D representations of the polynomial Eqs. (2)–(4). It can be observed that, as expected, the degradation rate improves as TiO_2 concentration increases, reaching the highest yield at around $1.8\,g\,L^{-1}$ thus confirming the positive influence of the increased number of TiO_2 active sites on the kinetics of the process. It is worthy to notice that in spite of their worse accuracy, analogous optimal TiO_2 concentrations were found at the three different response times evaluated. On the other hand, the wide range of pH values covered by the optimal response surface (red zone) indicates there is not a clear optimum pH in the experimental domain. Therefore, for practical purposes natural pH of the solution was selected, avoiding the addition of further reagents to the reaction. As it is later explained, these optimal conditions were fixed for the reaction performed to determinate atrazine photocatalytic degradation pathway.

3.2. Response surfaces of simazine degradation

Following an analogous methodology to that explained for atrazine degradation, the quadratic polynomial in terms of coded values (Eqs. (5)–(7)) were calculated for percent simazine degradation at 6, 10 and 15 min (response factors Y_1, Y_2 and Y_3, respectively) as follows:

$$Y_1 = 57.6874 + 4.9067\mathrm{pH} + 14.0850[TiO_2] - 7.0884\mathrm{pH}^2 - 6.9934[TiO_2]^2 - 0.4400\mathrm{pH}\cdot[TiO_2] \quad (5)$$

$$Y_2 = 82.3247 + 3.9867\mathrm{pH} + 16.0683[TiO_2] - 7.3068\mathrm{pH}^2 - 9.3218[TiO_2]^2 - 2.3525\mathrm{pH}\cdot[TiO_2] \quad (6)$$

$$Y_3 = 90.6989 + 2.4633\mathrm{pH} + 13.5400[TiO_2] - 5.8974\mathrm{pH}^2 - 7.5374[TiO_2]^2 - 3.8650\mathrm{pH}\cdot[TiO_2] \quad (7)$$

Similarly to atrazine, the P-values calculated by the ANOVA test indicated that the TiO_2 concentration is a significant factor in the model whereas pH is not. The response function coefficients (b_1 and b_2) show that pH and TiO_2 concentration have positive effects on simazine photocatalytic degradation. Table 4 displays the

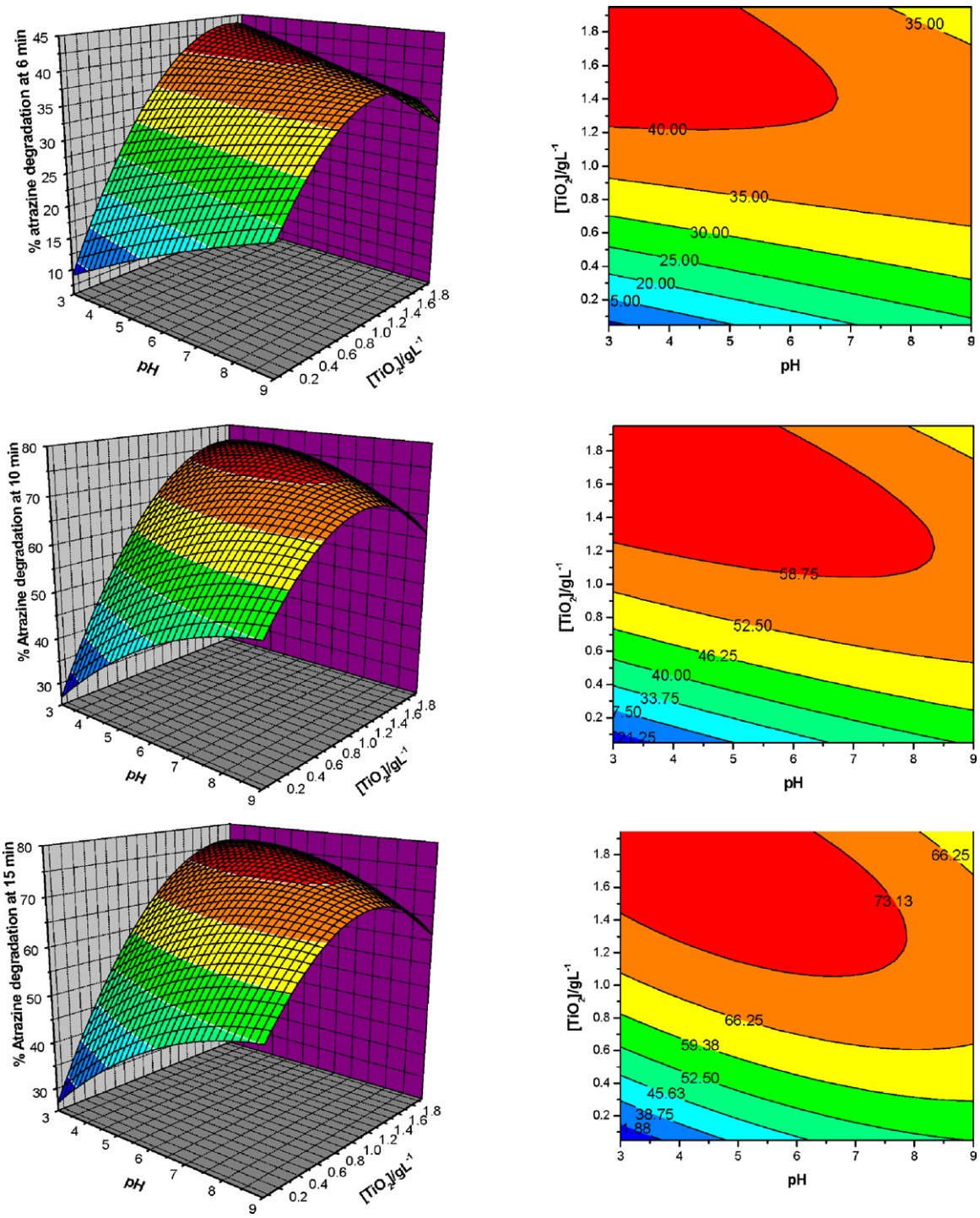

Fig. 2. Response surfaces and contour showing the effect of TiO_2 concentration and pH on the photocatalytic degradation of atrazine at 6, 10 and 15 min of irradiation.

experimental and predicted results for the three selected response factors.

The model explains the experimental range studied, as can be seen from the comparison of the graphical representation of experimental and predicted values in the Fig. 3. In this case, the values of R^2 obtained at 6, 10 and 15 min (0.9014, 0.9701 and 0.9512, respectively) are higher than found for atrazine therefore showing a better accuracy and indicating a reasonable predictability of the model.

The overall interaction effects are displayed in Fig. 4, which shows 3D and 2D representations of the polynomial Eqs. (5)–(7). It can be observed that, as expected, the degradation rate improves as TiO_2 concentration increases, reaching the highest yield at around 0.25 g L^{-1}. It is worthy to notice that analogous optimal TiO_2 concentrations were found at the three different response times evaluated. On the other hand, the optimum pH reached is the natural (around 5.5), although the wide range of pH values covered by the optimal response surface (red zone) indicates there is not a clear optimum pH in the experimental domain as it occurred for atrazine degradation.

At the sight of the experimental results, that seemed to indicate that increasing the titania concentration over the domain studied could result in an enhancement of the efficiency for simazine

Table 3
Experimental and calculated results from the factorial design of atrazine photocatalytic degradation.

No. Reaction	pH	TiO_2 concentration /g L^{-1}	Point of design	% Degradation at 6 min		% Degradation at 10 min		% Degradation at 15 min	
				Experimental	Predicted	Experimental	Predicted	Experimental	Predicted
1	6.0	1.00	(0,0)	36.3	37.9	54.4	57.9	57.9	72.1
2	3.0	0.05	(−1,−1)	7.3	9.1	12.8	51.3	20.0	26.7
3	6.0	0.05	(0,−1)	21.5	17.3	42.2	31.5	57.9	44.7
4	3.0	1.00	(−1,0)	36.7	36.4	55.8	55.9	69.3	64.4
5	6.0	1.00	(0,0)	40.6	37.9	60.0	57.9	73.1	72.1
6	6.0	1.00	(0,0)	35.1	37.9	54.0	57.9	66.7	72.1
7	9.0	1.95	(1,1)	32.6	31.7	50.7	81.9	63.2	61.2
8	9.0	0.05	(1,−1)	21.6	23.9	35.0	11.8	46.1	52.6
9	3.0	1.95	(−1,1)	45.0	43.5	66.2	34.4	78.1	76.3
10	9.0	1.00	(1,0)	39.4	37.9	61.0	59.9	74.2	69.7
11	6.0	1.95	(0,1)	36.0	38.4	53.0	58.2	70.0	73.8

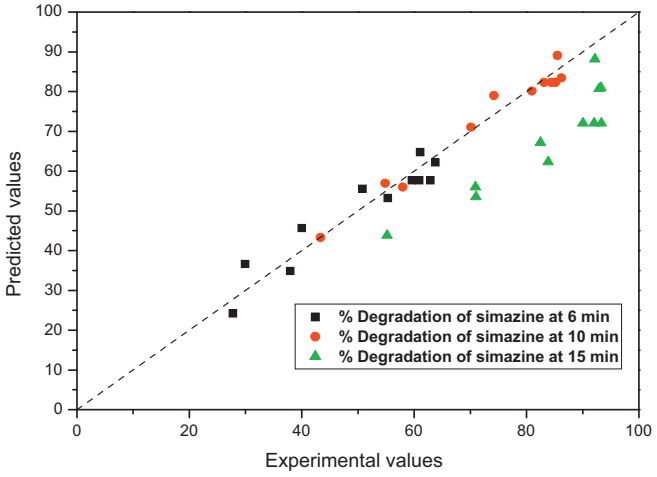

Fig. 3. Correlation between predicted and experimental values in the photocatalytic degradation of simazine at different irradiation times.

degradation, further experiments were performed at natural pH by increasing the concentration of TiO_2 to 0.5 and 1 g L^{-1}. The percentages of simazine degradation achieved after 15 min of irradiation were 73.9% and 75%, lower than those obtained within the 0.15–0.25 g TiO_2 L^{-1} range (Table 4).

3.3. Degradation pathway of atrazine

The mechanism of the photocatalytic degradation of atrazine was investigated by performing a reaction that lasted 40 h at the conditions above determined as optimal with the experimental design methodology (i.e., natural pH, 6.0, and a TiO_2 concentration of 1.8 g L^{-1}). Figs. 5 and 6 display the evolution of the concentration profiles of atrazine and detected degradation products as a function of irradiation time. Atrazine was degraded below detectable limits within the first 120 min of reaction but a mixture of C3 dealkylated products remained in the solution, even after 40 h of irradiation thus proving the difficulty for achieving the cleave of the triazine ring. According to the TOC measurements a 55% mineralization was achieved at the end of the reaction. The conversion of atrazine to the different C3 compounds detected at that time (Fig. 5) implies a maximum limit for TOC abatement of 62.5%, therefore the result obtained suggests that the complete oxidation of lateral alkyl chains was not achieved.

The intermediates identified at the first stage of the reaction indicate it initially proceeds through the removal of the isopropyl group yielding ACET, removal of the ethyl group forming ACIT or the replacement of the chlorine by a hydroxyl group, yielding EOIT. The last one attained a concentration in solution significantly higher than ACET and ACIT, therefore suggesting that hydroxylation of the chlorine site is a preferred initial pathway over the single dealkylation of atrazine. After peaking, dealkylated and dechlorinated products decreased in concentration, ACET and ACIT after 10 min whereas EOIT began to degrade after 90 min. These results show some dissimilarities with those reported by Héquet et al. [8] who also detected ACET, ACIT and EOIT as primary intermediates but found ACET as the major by-product followed by ACIT, being EEOT detected in low proportion. By contrast, Ta et al. [16] detected by LC–MS and GC–MS that the degradation product of atrazine by means of microwave-assisted electrodeless discharge mercury lamp was EOIT. Subsequent reactions of these intermediates yield

Table 4
Experimental results from the factorial design of simazine photocatalytic degradation.

No. Reaction	pH	TiO_2 concentration /g L^{-1}	Point of design	% Degradation at 6 min		% Degradation at 10 min		% Degradation at 15 min	
				Experimental	Predicted	Experimental	Predicted	Experimental	Predicted
1	5.5	0.15	(0,0)	60.9	57.7	84.4	82.3	93.3	72.1
2	3.0	0.05	(−1,−1)	27.8	24.2	43.3	43.3	55.2	43.9
3	5.5	0.05	(0,−1)	29.9	36.6	54.9	56.9	70.9	55.9
4	3.0	0.15	(−1,0)	40.0	45.7	70.1	71.0	83.9	62.3
5	5.5	0.15	(0,0)	62.9	57.7	85.1	82.3	92.0	72.1
6	5.5	0.15	(0,0)	59.6	57.7	83.1	82.3	90.0	72.1
7	8.0	0.25	(1,1)	63.7	62.2	86.2	83.4	93.2	80.9
8	8.0	0.05	(1,−1)	37.9	34.9	57.9	55.9	70.9	53.5
9	3.0	0.25	(−1,1)	55.3	53.2	80.9	80.1	92.9	80.7
10	8.0	0.15	(1,0)	50.8	55.5	74.2	79.0	82.5	67.2
11	5.5	0.25	(0,1)	61.1	64.8	85.5	89.1	92.2	88.1

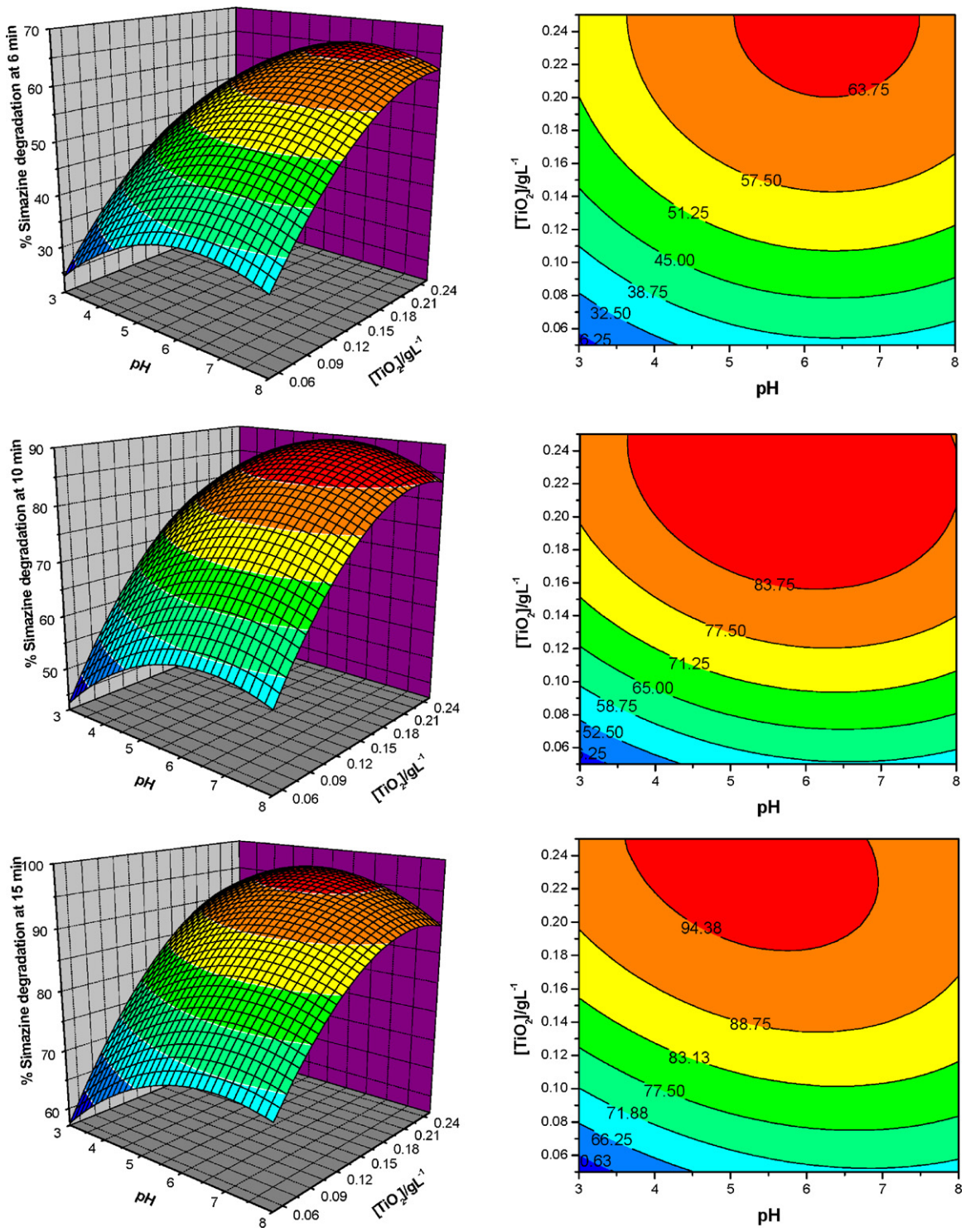

Fig. 4. Response surface and contour showing the effect of TiO_2 concentration and pH on the photocatalytic degradation of simazine at 6, 10 and 15 min of irradiation.

in first term AEOT, CAAT and AOIT, the latter in significantly less concentration than the former ones. The formation of AEOT could result from either the hydrolysis of chlorine substituent in ACET or by removal of isopropyl group from EOIT. CAAT can be formed from removal of alkyl side chains of either ACET or ACIT. The removal of ethyl group from EOIT or the hydrolysis of chlorine substituent in ACIT would account for the formation of AOIT. It should be noticed the profile of CAAT concentration, as it decreases more gradually than the alkylated intermediates. In fact, it was still present in the solution after 40 h of irradiation. Ammeline, ammelide and cyanuric acid, products formed upon removal of both side alkyl chains and progressive hydroxylation of the s-triazines ring, were also identified. It should be mentioned that it was detected the formation of an intermediate contemporary to the appearance of ammeline and ammelide, whose concentration increased along the reaction. This compound was also produced upon oxidation of ammelide with $KMnO_4$, therefore it is reasonable to consider it is a nitro derivative of atrazine, most likely 2,4-dihydroxy-6-nitroatrazine. No reference standard was commercially available, for that reason no quantification of concentration of this intermediate could be done.

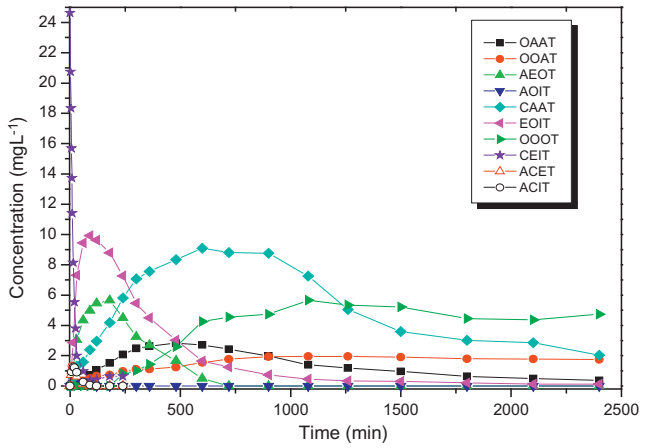

Fig. 5. Concentration profiles and intermediates in the degradation of atrazine (25 mg L^{-1}).

Finally, to get further information about the last stage of the photocatalytic degradation of atrazine, two reactions at an initial concentration of 15 mg L^{-1} of ammeline and 15 mg L^{-1} ammelide were carried out for 76 and 90 h, respectively. Figs. 7 and 8 depict the evolution of concentration profiles as a function of irradiation time. As it can be observed, photocatalytic degradation of ammeline yielded ammelide and cyanuric acid as main products. In the case of ammelide degradation, cyanuric acid could be identified as main product of the reaction. It should be noticed, however, that also formation of 2,4-dihydroxy-6-nitroatrazine was detected in both reactions. It has been previously proposed that the formation of cyanuric acid as final product of the photocatalytic degradation of atrazine follows the sequence OAAT → OOAT → OOOT [8] although, on the other hand, Minero et al. [7] found that under solar irradiation ammelide was not formed through ammeline. Formation of cyanuric acid from photocatalytic degradation of ammeline and ammelide has been confirmed by the reactions performed with both molecules as parent compounds. However, the comparison of concentration profiles shown in Figs. 7 and 8 with those displayed in Fig. 5 evidence that the progression OAAT → OOAT → OOOT is not the only pathway for cyanuric acid formation from atrazine degradation. One plausible explanation should be an additional path to yield cyanuric acid through the progressive hydroxylation of CAAT by displacement of the amino group in first place followed by a further displacement of the chlorine group. The results discussed above are summarized in the proposed degradation pathway for atrazine photocatalytic degradation shown in Fig. 9 (dotted arrows indicate the products have not been undoubtedly identified but are likely to be formed).

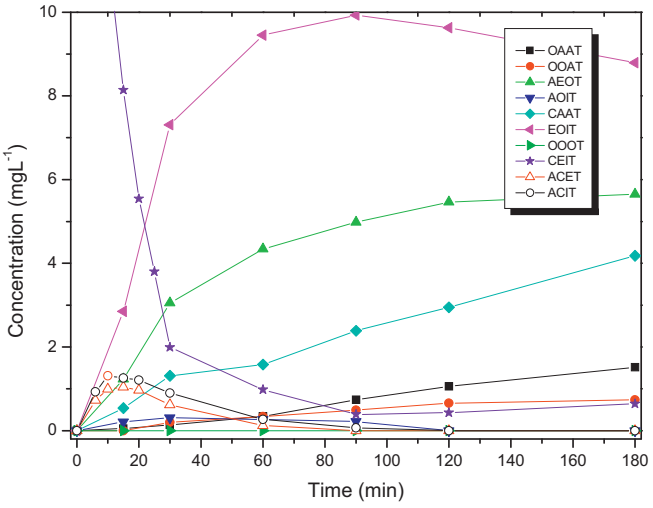

Fig. 6. Enlargement of Fig. 5.

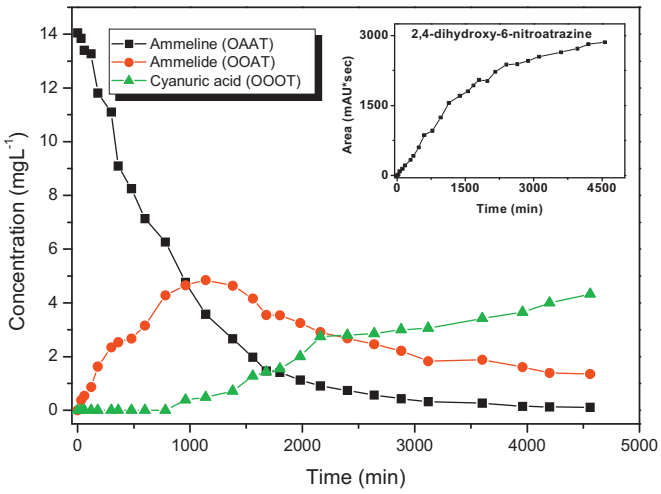

Fig. 7. Concentration profiles in the photocatalytic degradation of ammeline (15 mg L^{-1}). In the inset: HPLC peak area of 2,4-dihydroxy-6-nitroatrazine as a function of the irradiation time.

3.4. Degradation pathway of simazine

Following an analogous procedure than for atrazine, the mechanism of the photocatalytic degradation of simazine was investigated. A photocatalytic reaction at the optimal conditions obtained from the experimental design (natural pH, 5.5, and 0.25 g L^{-1} of TiO_2) was carried out for 40 h. A fast disappearance of simazine (95% removal in 15 min) could be observed but no full mineralization of the herbicide was achieved. The much lower initial concentration of simazine (5 mg L^{-1}) determined by its lower solubility and the symmetry of alkyl side chains lead to the detection of a less number of intermediates as compared to atrazine degradation. Moreover, as the concentration of intermediates formed along the reaction was quite close to the detection limit of the chromatography method employed, a rigorous quantitative analysis could not be performed in this case. The primary path-

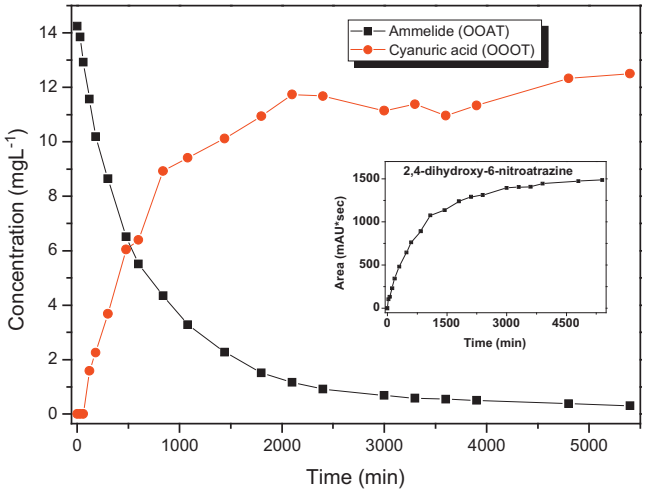

Fig. 8. Concentration profiles in the photocatalytic degradation of ammelide (15 mg L^{-1}). In the inset: HPLC peak area of 2,4-dihydroxy-6-nitroatrazine as a function of the irradiation time.

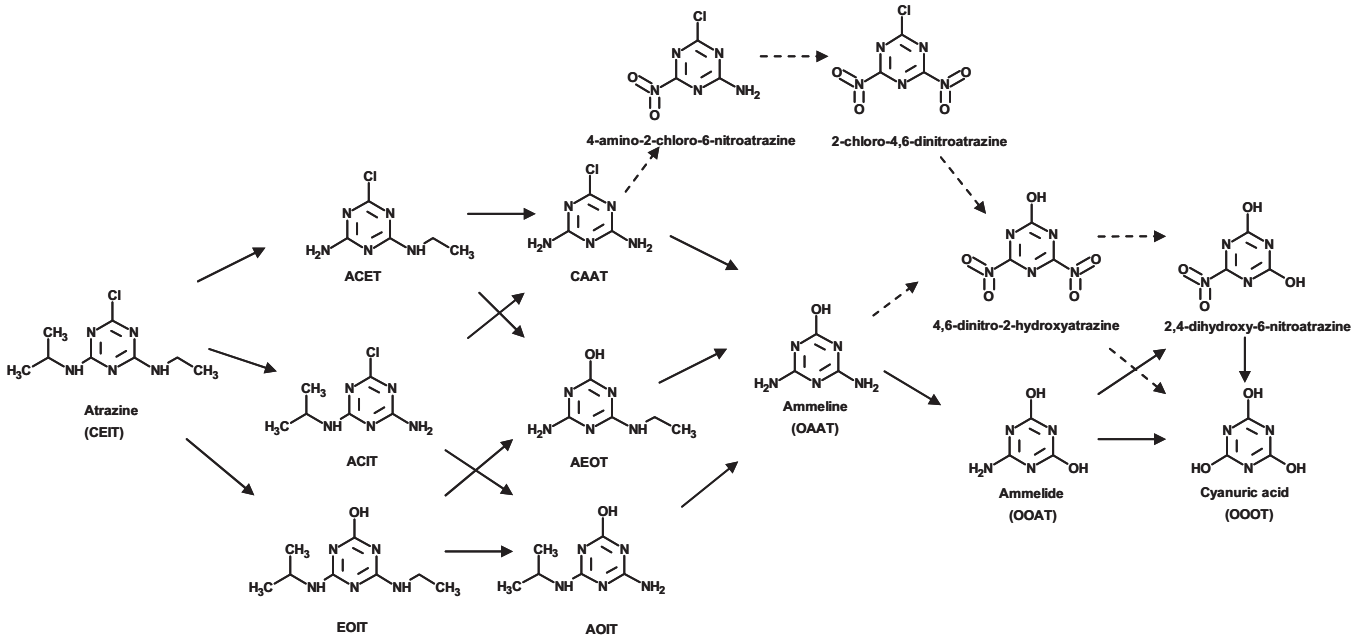

Fig. 9. Scheme of proposed pathway for atrazine photocatalytic degradation.

way for simazine photocatalytic degradation involved dealkylation (alkylic side chain cleavage) and dechlorination (hydroxylation of the chlorine site) processes, according to the detection of CAAT and AEOT. The major concentration of CAAT points out a preferential pathway for dealkylation of simazine. Ammeline, ammelide and cyanuric acid were detected following similar reaction profiles as seen for atrazine degradation. Finally, it should be mentioned the formation of EEOT at the first stage of the reaction although below quantifiable limits, and that the peak attributable to 2,4-dihydroxy-6-nitroatrazine was also observed to increase in the chromatograms registered along the reaction time. On the basis of detected products, the reaction mechanism shown in Fig. 10 is proposed.

3.5. Toxicity assessments

The toxicity of samples withdrawn along the photocatalytic reactions was evaluated by monitoring changes in the natural emission of the luminescence bacteria *Vibrio fischeri* as explained in the experimental.

Fig. 11 displays the percentage of inhibition of bacteria as a function of irradiation time for atrazine and simazine photocatalytic degradation. The values of inhibition after 15 min of *Vibrio fischeri* contact to atrazine and simazine initial solutions were 82% and 73%, respectively. As the reaction progressed, toxicity was reduced reaching at the end of the run inhibition values of 31% for atrazine and 46% for simazine. The evolution of toxicity of the samples obtained from ammeline and ammelide reactions was also investigated. Inhibition percentages of 42% and 33% were respectively measured for the initial solutions of ammeline and ammelide. In the first case, for which a mixture of ammelide and cyanuric acid was present after 76 h of irradiation the percentage of inhibition was reduced to 27%. By contrast, in the case of the reaction of ammelide, where only cyanuric acid remained as final stable product, the toxicity decreased reaching a final value of less than 1%. The results indicate that the toxicity of

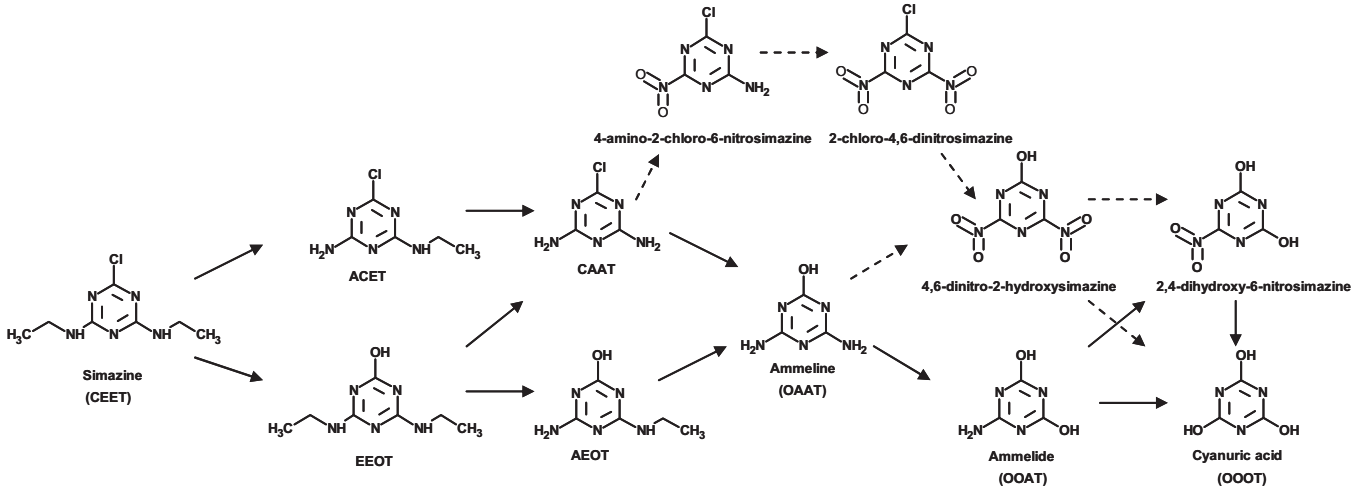

Fig. 10. Scheme of proposed pathway for simazine photocatalytic degradation.

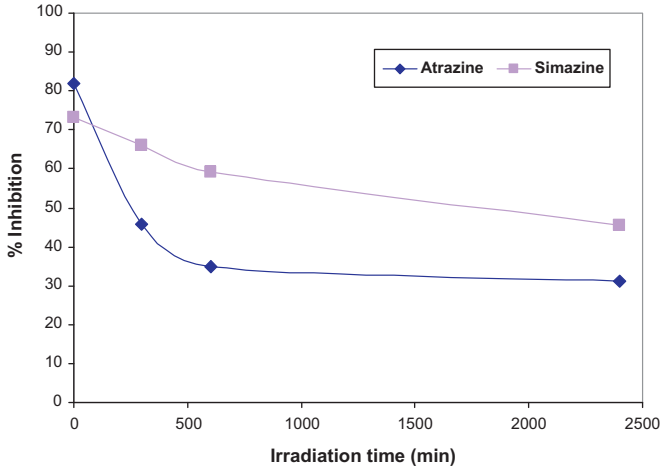

Fig. 11. Results of toxicity in the triazine samples when optimal variables were used.

the herbicides solutions decreases as formation of hydroxylated compounds increases, reaching the lowest value for cyanuric acid solutions.

4. Conclusions

Design of experiments has been used in order to evaluate the influence of pH and TiO_2 concentration on the atrazine and simazine photocatalytic degradation. Response surfaces have been obtained for each s-triazine studied. The mathematical models obtained have shown that TiO_2 concentration has significant influence on the degradation efficiency in contrast to pH that has a scarce influence on the degradation performance.

Determination of main intermediates formed during the photocatalytic degradation of both herbicides has probed it is not achieved the complete mineralization, being cyanuric acid the main stable product. Based on the evolution of the concentration profiles of the intermediates pathways for atrazine and simazine photocatalytic degradation have been proposed. The reaction proceeds through dealkylation and dechlorination steps for both herbicides leading to the highly hydroxylated intermediates, ammeline, ammelide and cyanuric acid. Also, it is proposed that besides hydroxylation of ammelide and ammeline, cyanuric acid can be formed from nitro-atrazine/simazine derivatives resulting by the oxidation of the amine groups of ammeline and ammelide.

The toxicity along the reaction has been monitored by means of luminescence bioassays using *Vibrio fischeri*. The inhibition percentage decreases with the irradiation times what can be associated with the formation of highly hydroxylated intermediates.

Acknowledgements

The authors thank the regional government of Madrid that has financed this work through the research project "REMTAVARES" (S-2009/AMB/1588) and to the "Ministerio de Ciencia e Innovación" for the financial support through the projects CTQ2006-04720, CTM2009-08649 and "CONSOLIDER INGENIO 2010" (CSD2006-44). Asunción Revilla thanks to "Ministerio de Ciencia e Innovación" the FPI grant.

References

[1] M. Radosevich, S.J. Traina, Y. Hao, O.H. Tuovinen, Am. Soc. Microbiol. 61 (1995) 297.
[2] M. Graymore, F. Stagnitti, G. Allinson, Environ. Int. 26 (2001) 483.
[3] Directive 2000/60/EC of the European Parliament and of the Council of October 23, 2000 establishing a framework for Community action in the field of water policy (L327 of 22-12-2000) and Directive 2008/105/EC of the European Parliament and of the Council of December 16, 2008 on environmental quality standards in the field of water policy, amending and subsequently repealing Council Directives 82/176/EEC, 83/513/EEC, 84/156/EEC, 84/491/EEC, 86/280/EEC and amending Directive 2000/60/EC of the European Parliament and of the Council (L348 of 24-12-2008).
[4] S. Parra, J. Olivero, C. Pulgarín, Appl. Catal. B: Environ. 36 (2002) 75.
[5] S. Malato, J. Blanco, J. Cáceres, A.R. Fernández-Alba, A. Agüera, A. Rodríguez, Catal. Today 76 (2002) 209.
[6] E. Pelizzetti, V. Maurino, C. Minero, V. Carlin, E. Pramauro, O. Zerbinati, M.L. Tosato, Environ. Sci. Technol. 24 (1990) 1559.
[7] C. Minero, E. Pelizzetti, S. Malato, J. Blanco, Sol. Energy 56 (1996) 411.
[8] V. Héquet, C. González, P. le Cloirec, Water Res. 56 (2001) 4253.
[9] T.A. McMurray, P.S.M. Dunlop, J.A. Byrne, J. Photochem. Photobiol. A: Chem. 182 (2006) 43.
[10] W. Chu, Y. Rao, W.Y. Hui, J. Agric. Food Chem. 57 (2009) 6944.
[11] E. Pelizzetti, C. Minero, M. Vincenti, E. Pramauro, Chemosphere 24 (1992) 891.
[12] J. Fernández, J. Kiwi, J. Baeza, J. Freer, C. Lizama, H.D. Mansilla, Appl. Catal. B: Environ. 48 (2004) 205.
[13] G.E.P. Box, W.G. Hunter, J.S. Hunter, Statistics for Experimenters, Design, Innovation, and Discovery, John Wiley and Sons, New Jersey, 1978.
[14] A.M. Cook, R. Hütter, J. Agric. Food Chem. 29 (1981) 1135.
[15] S. Nélieu, L. Kerhoas, J. Einhorn, Environ. Sci. Technol. 34 (2000) 430.
[16] N. Ta, J. Hong, T. Liu, C. Sun, J. Hazard. Mater. B138 (2006) 187.